

## Article

# Theoretical Study and Adsorption Behavior of Urea on Mild Steel in Automotive Gas Oil (AGO) Medium

Nleonu Emmanuel Chile <sup>1,†</sup>, Rajesh Haldhar <sup>2,†</sup>, Ubaka Kelechi Godfrey <sup>1</sup>, Onyemenonu Christopher Chijioke <sup>1</sup>, Ezeibe Anderson Umezuruike <sup>1</sup>, Okeke Pamela Ifeoma <sup>3</sup>, Mong Oke Oke <sup>4</sup>, Hamza Ichou <sup>5</sup>, Nadia Arrousse <sup>6,\*</sup>, Seong-Cheol Kim <sup>2,\*</sup>, Omar Dagdag <sup>7</sup>, Eno E. Ebenso <sup>7</sup> and Mustapha Taleb <sup>6</sup>

- <sup>1</sup> Chemistry Department, Federal Polytechnic Nekede, Owerri 460114, Nigeria; enleonu@yahoo.com (N.E.C.); ubakakelechi09@gmail.com (U.K.G.); conyemenonu@fpno.edu.ng (O.C.C.); kingibe76@yahoo.com (E.A.U.)
- <sup>2</sup> School of Chemical Engineering, Yeungnam University, Gyeongsan 38541, Korea; rajeshhaldhar.lpu@gmail.com
- <sup>3</sup> Department of Basic Science, Alvan Ikoku College of Education, Owerri 460114, Nigeria.; okekepamelaify@gmail.com
- <sup>4</sup> Department of Mechanical Engineering, Federal Polytechnic Nekede, Owerri 460114, Nigeria; omong@fpno.edu.ng
- <sup>5</sup> Centre d'élaboration de Matériaux et d'études Structurales, Université Toulouse III, UPS, 118 Route Narbonne, F-31062 Toulouse, France; ichou.hamzaqm@gmail.com
- <sup>6</sup> Laboratory of Engineering, Organometallic, Molecular and Environment (LIMOME), Faculty of Science, University Sidi Mohamed Ben Abdellah, Fez 1796, Morocco; mustaphataleb62@yahoo.fr
- <sup>7</sup> College of Science, Engineering and Technology, University of South Africa, Johannesburg 1710, South Africa; omar.dagdag@uit.ac.ma (O.D.); ebensee@unisa.ac.za (E.E.E.)
- \* Correspondence: nadiarrousse@gmail.com (N.A.); sckim07@ynu.ac.kr (S.-C.K.)
- † These authors contributed equally to this work.



**Citation:** Chile, N.E.; Haldhar, R.; Godfrey, U.K.; Chijioke, O.C.; Umezuruike, E.A.; Ifeoma, O.P.; Oke, M.O.; Ichou, H.; Arrousse, N.; Kim, S.-C.; et al. Theoretical Study and Adsorption Behavior of Urea on Mild Steel in Automotive Gas Oil (AGO) Medium. *Lubricants* **2022**, *10*, 157.

<https://doi.org/10.3390/lubricants10070157>

Received: 20 June 2022

Accepted: 10 July 2022

Published: 14 July 2022

**Publisher's Note:** MDPI stays neutral with regard to jurisdictional claims in published maps and institutional affiliations.



**Copyright:** © 2022 by the authors. Licensee MDPI, Basel, Switzerland. This article is an open access article distributed under the terms and conditions of the Creative Commons Attribution (CC BY) license (<https://creativecommons.org/licenses/by/4.0/>).

**Abstract:** The continuous search for eco-friendly corrosion inhibitors due to differences in corrosive media remains an important point in corrosion control. The experimental studies on the corrosion inhibition of urea on mild steel in automotive gas oil (AGO) was conducted using gasometric techniques and scanning electron microscope (SEM). The theoretical approach on the density functional theory (DFT) on the urea molecule was carried out using Gaussian 09 software. The adsorption behavior of urea molecules on the surface of the mild steel was analyzed using Frumkin and Flory-Huggins adsorption isotherms models and Gibb's free energy, respectively. The result of the experimental study shows a poor corrosion inhibitory effect of urea on mild steel in automobile gas oil (AGO) medium as the inhibition efficiency decreased from 69.30% in week 1 to 12% in week 11 at 200 ppm of inhibitor. The adsorption of urea on the mild steel surface obeys Frumkin's adsorption isotherm model. Gibb's free energy of adsorption of urea molecules onto mild steel surface revealed a physisorption mechanism. SEM results showed the non-inhibitive nature of urea on the studied mild steel. Quantum chemical parameters such as HOMO, LUMO, electron affinity, electronegativity, and the fraction of electrons transferred to the metal surface were calculated and interpreted to compare the experimental and theoretical results. The theoretical findings in the current investigation were not in agreement with the experimental result, thereby creating a need for further study using the electrochemical method.

**Keywords:** mild steel; adsorption behavior; automotive gas oil; corrosion inhibition; quantum chemical parameters

## 1. Introduction

Pipelines are extremely important in industrial application in the transportation of petroleum products over long distances from their sources to the destination [1]. Pipelines are sometimes buried underground and only make their presence known at the stations [1].

The most used material in oil and gas industries is mild steel because of its ductility, strength, weldability, durability, corrosion resistance, thermal expansion, and its resistance to heat treatment for varying mechanical properties [2,3]. In the petroleum industry, corrosion is a major nightmare as mild steel pipelines play the role of transporting oil and gas from wellheads to the processing facilities and they are exposed to the continuous threat of corrosion from the date of commissioning up to decommissioning or abandonment [4]. Corrosion inhibitors are an original way of combating corrosion.

The originality of this method stems from the nature of the anticorrosion treatment, which does not operate on the metal itself but through the corrosive medium on the metal itself. The inhibition of corrosion by organic compounds is one of the various alternatives for combating this phenomenon. The action of these compounds essentially results from their adsorption on the metal surface, and the formation of a nonsoluble and adherent protective film on the surface of the metal. Preventing the access of the corrodent depends largely on the structural and electronic properties of the compounds intended to be used as corrosion inhibitors [5].

Indeed, most of the organic inhibitors used in an acidic environment have aromatic rings, multiple bonds (single and double), and/or heteroatoms in their structures such as nitrogen, oxygen, sulphur, or phosphorus, which gives them a high reactivity to adsorb onto the material surface.

Traditionally, the evaluation of inhibition performance is mainly carried out experimentally by gravimetric and electrochemical methods coupled with surface analysis techniques [6]. However, these experimental techniques remain insufficient to fully understand the mechanism of action of an inhibitor. Therefore, corrosion studies have turned to the exploitation of theoretical chemistry to explain the mechanisms of inhibition. Such an approach, based on the study of the intrinsic properties of the systems studied, has shown its validity as an innovative and extremely promising approach [7].

Corrosion has led to damage in pipelines, which are usually costly to repair, costly in terms of loss or contamination of product, environmental damage, and possibly to human safety [8]. The fluids in the pipeline are responsible for corrosion. Carbon dioxide (CO<sub>2</sub>) and hydrogen sulphide (H<sub>2</sub>S) gases in the presence of water are also major sources of corrosion in oil and gas production [9–11]. Hydrogen sulfide is known to pose a serious risk of damage to metals and their compounds in oil and gas environments. Hydrogen sulfide is a weak acid that is soluble in water and is part of many chemicals in oils and pipelines. The mechanism of the entire process is as follows [12]:



Iron sulfide formation is the product of corrosion. The carbon dioxide that is produced along with oil and gas dissolves in water to form carbonic acid, which reacts with mild steel pipeline causing corrosion damage [12]:



The formed iron carbonate is the corrosion product and usually reduces the corrosion rate. Corrosion prevention and control are of great importance in petroleum industries. One way of overcoming corrosion on metals is the use of corrosion inhibitors [13–15]. Corrosion inhibitors have been recognized as one of the preventive measures of corrosion control in petroleum industries [16,17]. Over the years, corrosion engineers and scientists have been working towards designing and synthesizing eco-friendly and effective corrosion inhibitors [18]. Consequently, organic inhibitors of various classes have been a major subject

of research interest as potential materials for the surface protection of ferrous metals and their alloys in different aggressive environments [19,20].

Urea is an organo-oxygen compound with the formula  $\text{CO}(\text{NH}_2)_2$ . The presence of nitrogen and oxygen makes urea an effective corrosion inhibitor [21]. Organic inhibitor compounds containing heteroatoms such as nitrogen, oxygen, sulphur, or phosphorous in a conjugated system have been identified to possess excellent corrosion inhibiting properties as corrosion inhibitors [22,23]. Inhibition by organic compounds form strong film protection on the surface of the mild steel through the adsorption process [24,25].

There is a shortage of literature on utilization of organic inhibitors for inhibition of mild steel in petroleum products. The purpose of this work is to evaluate the inhibition potential of urea in controlling corrosion of mild steel immersed in automotive gas oil (AGO) media by studying hydrogen evolution and scanning electron microscopy micrographs. Quantum chemical computations were conducted using density functional theory (DFT).

## 2. Materials and Methods

### 2.1. Materials

Urea ( $\text{OC}(\text{NH}_2)_2$ ) was a product of Sigma Aldrich with 98% purity and was used without further purification. Hence, 200 ppm of urea was utilized in this study because previous studies have reported that urea has high inhibition efficiency at low concentration and loses its efficiency at high concentration [26]. The corrosive environment in the investigation was AGO, which was purchased from Mega Filling Station located along Owerri—Aba Road, Imo state, Nigeria. The chemical structure of urea is displayed in Figure 1. The physicochemical properties of the corrodent (AGO) are shown in Table 1.

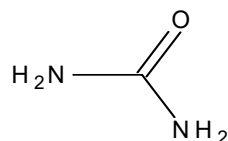


Figure 1. Molecular structure of urea.

Table 1. Chemical composition of the studied mild steel (MS).

Atoms	Fe	Ca	P	S	O	K	Mg	Na	Al	Si	Mo	C
Content (%)	95.23	0.20	0.20	0.23	0.26	0.25	0.25	0.35	0.35	0.39	0.69	1.61

### 2.2. Preparation of the Mild Steel

The studies were carried out on mild steel, and the chemical composition obtained with the use of energy dispersive spectroscopy (EDX) is shown in Table 1. Coupons with dimensions of 2.0 cm × 2.0 cm with thickness of 0.041 cm<sup>3</sup> with surface area of 8.0 cm<sup>3</sup> were used in the corrosion study. The coupons were polished with sic emery paper, degreased with ethanol, washed with acetone, dried with warm air, and stored in moisture free desiccator prior to the experiment.

### 2.3. Gasometric Measurement

The gasometric method described in our previous work was adopted without further modification for the corrosion study [20]. Hydrogen evolution measurements were carried out using gasometric assembly. Then 200 cm<sup>3</sup> of AGO was introduced into the reaction vessel connected to the gasometric assembly and the initial volume of air paraffin oil in the burette was recorded. Then the mild steel coupon was dropped into the corrodent and the reaction flask quickly closed to prevent leakage of hydrogen gas. The change in the volume of hydrogen gas evolved with time and was recorded every week by noting the volume change in the level of paraffin oil in the burette for 12 weeks. Furthermore, the mild steel coupon was immersed in 200 cm<sup>3</sup> of the AGO medium containing 200 ppm of

urea for 12 weeks. The change in the volume of paraffin oil in the presence and absence of urea was used to monitor the corrosion of mild steel. The corrosion rates of the mild steel was calculated using following equation:

$$\text{Corrosion rate (mpy)} = \frac{534 H}{\rho AT} \quad (5)$$

where H is the hydrogen gas evolution in (mL),  $\rho$  is the metal density in  $\text{g/cm}^3$ , A is the exposed area of the mild steel in  $\text{cm}^2$ , and T is the exposure time in hours.

Then the percentage inhibition efficiency (%IE) and surface coverage ( $\theta$ ) were calculated using following equations:

$$\% \text{ IE} = \frac{\text{CR}_{\text{blank}} - \text{CR}_{\text{inh}}}{\text{CR}_{\text{blank}}} \times 100 \quad (6)$$

$$\theta = \frac{\text{CR}_{\text{blank}} - \text{CR}_{\text{inh}}}{\text{CR}_{\text{blank}}} \quad (7)$$

where  $\text{CR}_{\text{blank}}$  and  $\text{CR}_{\text{inh}}$  are corrosion rate with and without urea inhibitor, respectively.

#### 2.4. Surface Examination Study

The defensive layer was formed on the mild steel surface when the corrosion test was analyzed by scanning electron microscopy (SEM) combined with the EDX analysis. Estimations of the morphology of the mild steel were inspected with a phenom proxcomputer-controlled SEM instrument.

#### 2.5. Computational Investigation

##### 2.5.1. DFT Calculations

The quantum chemistry calculations of the urea molecule including complete geometrical optimization were performed by density functional theory (DFT) method at B3LYP and 6–31 G as the basis set utilizing Gaussian 09. The energies of the highest occupied molecular orbital ( $E_{\text{HOMO}}$ ) and lowest unoccupied molecular orbital ( $E_{\text{LUMO}}$ ) were determined and examined. Different theoretical parameters, for example, the fraction of electron transferred ( $\Delta N$ ), global electrophilicity ( $\omega$ ), softness ( $\sigma$ ), energy gap ( $\Delta E$ ), nucleophilicity ( $\epsilon$ ), electronegativity ( $\chi$ ), and hardness ( $\eta$ ) have been determined following relevant equations [27].

##### 2.5.2. MC Simulation

The Monte Carlo model was utilized to acquire the accessible information on the conduct of inhibitors contemplated during the adsorption on the mild steel surface [28]. Here, the impact with Fe (110) was identified and tested using the Studio 2017 program kit [29]. The optimized inhibitor molecule was adsorbed on the surface of Fe (110) within the sight of 100 water molecules, which impacted the steadiest adsorbed arrangement of the examined inhibitor on the surface of material studied with higher negative adsorption energy values [30].

#### 2.6. Property Test of Automotive Gas Oil (AGO)

The physicochemical properties of AGO were tested using the standard test method [27,28]. Table 2 shows the physicochemical properties of AGO.

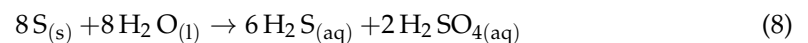
**Table 2.** Physicochemical properties of automotive gas oil (AGO).

Parameters	AGO
pH	7.01
Conductivity ( $\mu\text{S}/\text{cm}^3$ )	0.00
Carbon (ppm)	85.70
Sulphur (ppm)	236.41
Density (g/mL)	0.8191

### 3. Results and Discussion

#### 3.1. Corrosive Properties of AGO

The results regarding the corrosive properties of automotive gas oil are given in Table 1. The results show neutral nature and nonionic salt in the corrodents. The sulphur content was 236.41 ppm. Crude oil and its products contain different types of sulphur compounds such as mercaptans, thiophenes, and elemental sulphur [29]. Corrosion of metal surfaces due to direct interaction of sulphur and metal is known as localized corrosion. The general chemical reaction between sulphur and metal is given in these equations:



These theoretical explanations concerning the nature of the corrosion of ferrous metals in AGO can be used to predict the possible mechanisms for the formation of FeS as products of corrosion by mild steel in oil and gas environments.

#### 3.2. Corrosion Study

The rate of metal degradation and reticence effectiveness during immersion is shown in Figures 2 and 3, respectively. It was found that the immersion time increased from 1 week to 11 weeks with decreasing reticence effectiveness, confirming the inefficiency of urea. However, the recorded inhibition efficiency observed in week one was not sustained with the rise in immersion time. This behaviour suggests that adsorption of urea molecules on the mild steel surface occurred via physical means and adsorbed protective film dissolves with an increase in contact time resulting in exposing some protected surfaces to corrosion attack [31]. The poor inhibitory effect may also be attributed to the nature of interaction between the inhibitor molecules and the metal surfaces [32]. Furthermore, the result obtained in this study was in agreement with the decrease in inhibitory effect of 4-benzyl-1-(4-oxo-4-phenylbutanoyl) thiosemicarbazide on the corrosion of mild steel in 1.0 M HCl when the exposure period increased from 10 to 48 h [33]. The outcome of inhibition efficiency and corrosion rate shows ineffective reticence abilities of urea for the mild steel in AGO environment.

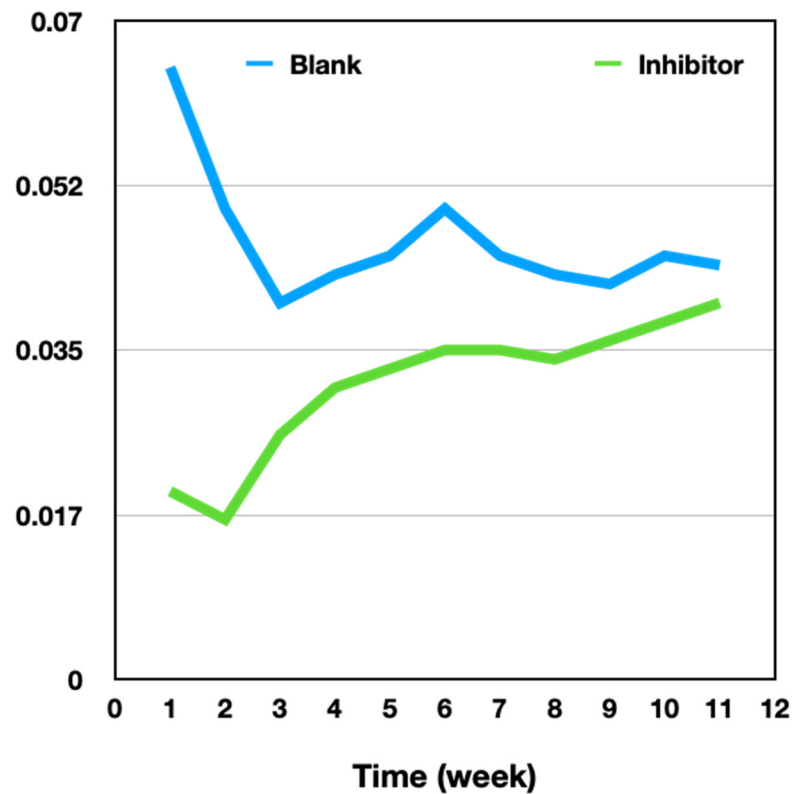


Figure 2. Variation of corrosion rate in the presence and absence of inhibitor.

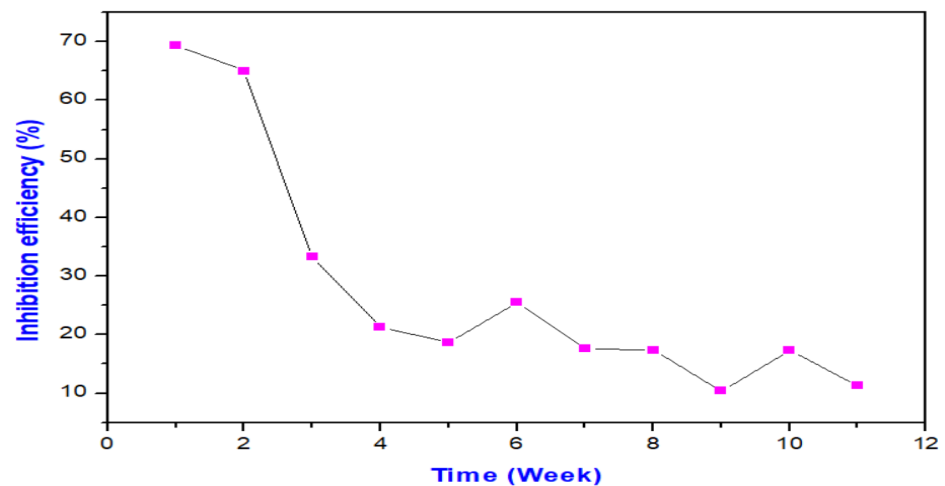


Figure 3. Variation of inhibition efficiency of urea inhibitor with time.

### 3.3. Adsorption Study

Adsorption isotherms are very interesting models in order to understand how inhibitive the protected material was from corrosion [30]. The fitness of experimental data was tested on Flory-Huggins and Frumkin adsorption isotherms to comprehend the adsorption properties of urea onto the metal surface using the degree of surface coverage ( $\theta$ ) parameters. The linear equations of each isotherm were used to model the isotherms [20].

Flory-Huggins isotherm:

$$\log\left(\frac{\theta}{C_{\text{inh}}}\right) = \log k + x \log(1 - \theta) \quad (12)$$

Frumkin isotherm:

$$\ln C_{\text{inh}} \left( \frac{\theta}{C_{\text{inh}}} \right) = \ln k + 2d\theta \quad (13)$$

where  $x$  constitute the amount of adsorbed water molecules removed by one inhibitor molecules,  $d$  represents the interaction factors among adsorbed molecules (repulsion or attraction force), and  $K$  is the equilibrium constant.  $K$  is obtained from the intercept of the linear graph while  $x$  and  $d$  are obtained from the slope of the linear graph.

The adsorption equilibrium constants ( $K$ ) in the system are related to standard Gibb's free energy of adsorption ( $\Delta G_{\text{ads}}$ ) by the following equation [20]:

$$\Delta G_{\text{ads}}^{\circ} = -2.303RT \log 55.5K_{\text{ads}} \quad (14)$$

where the parameters retain their standard meaning.

The obtained values of the adsorption isotherms and standard Gibb's free energy of adsorption are presented in Table 3. The calculated  $\Delta G_{\text{ads}}^{\circ}$  from Frumkin adsorption parameter is  $-17.30$  KJ/mol. In the present study, the calculated value of  $\Delta G_{\text{ads}}^{\circ}$  at 303 K was close to  $-20$  KJ/mol indicating electrostatic interaction and physisorption adsorption between the inhibitor and the charged metal surface. This implies that the film formation by the inhibitor on the surface of the metal was spontaneous.

**Table 3.** Parameters issue from adsorption isotherm models and standard Gibb's free energy values for the adsorption of urea on mild steel surfaces in AGO media.

Frumkin Isotherm	Values	Flory-Huggins Isotherm	Values
$R^2$	0.9821	$R^2$	0.8751
$d$	2.4077	$X$	$-1.5951$
$K_{\text{ads}}$	17.30	$K_{\text{ads}}$	$6.26 \times 10^{-2}$
$\Delta G_{\text{ads}}^{\circ}$ (kJ / MNI)	$-17.30$	$\Delta G_{\text{ads}}^{\circ}$ (KJ/MNI)	8.00

### 3.4. Surface Analysis

Following a month of immersion, the mild steel surfaces were inspected with and without the urea inhibitor to obtain access to data on the adsorption conduct of the inhibitor on the substance [34]. Scanning electron microscopy (SEM) micrographs and EDX patterns are displayed in Figures 4 and 5, respectively. The surface area of mild steel within the sight of urea immersed in AGO appears more damaged than the mild steel immersed in AGO without inhibitor, because of localized corrosion onto the protected material surface. The energy dispersive X-ray (EDX) attached to the SEM was applied to detect the mild steel impurities and other chemical elements except iron; as well as the component of the inhibitor used to fight against corrosion of the mild steel before and after immersion in AGO with and without urea inhibitor. The level of atomic qualities for various molecules and mild steel is displayed in Table 4. This is shown by the values of percentage weight in atomic composition of mild steel where the urea inhibitor does not respond after drenching and does not restrain hindrance against the mild steel because of corrosive media.

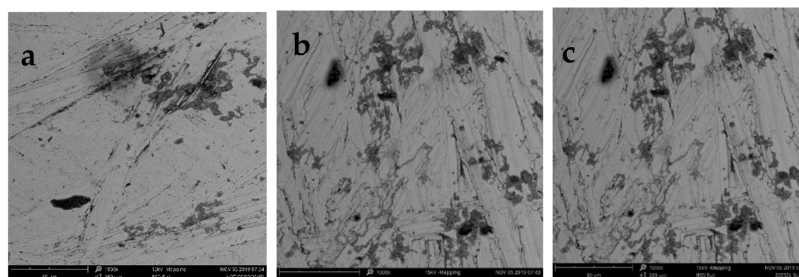


**Figure 4.** SEM micrograph of: (a) mild steel coupon before immersion, (b) exposed to AGO in absence of urea, and (c) exposed to AGO in the presence of urea.

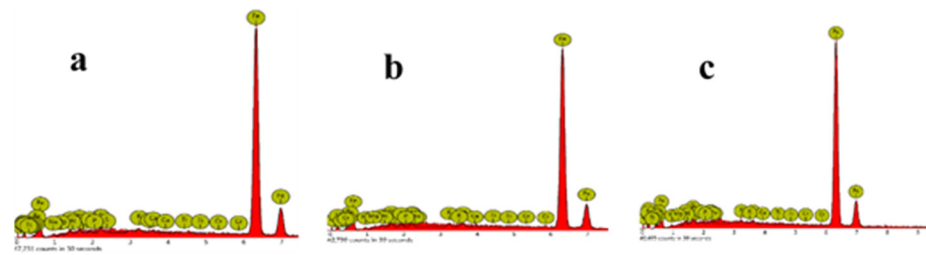


**Figure 5.** EDX pattern of mild steel: (a) before immersion, (b) exposed to AGO in the absence of urea, and (c) exposed to AGO in the presence of urea. (Counts in 30s).

**Table 4.** Percentage weight composition of elements obtained from SEM-EDX analysis.

Elements	Pure Mild Steel	Mild Steel in AGO	Mild Steel in AGO and Inhibitor
Fe	95.23	94.53	93.81
C	1.61	1.69	3.23
Mo	0.69	0.00	0.00
Si	0.39	0.49	0.64
Al	0.35	0.22	0.42
Na	0.35	0.33	0.27
K	0.26	0.50	0.21
Mg	0.25	0.17	0.09
o	0.24	0.33	0.35
S	0.23	0.45	0.22
P	0.20	0.36	0.19
Ca	0.20	0.59	0.25
Cr	0.00	0.15	0.18
Ti	0.00	0.20	0.13

### 3.5. Theoretical Approach

The theoretical approach has been utilized to comprehend the interaction between the organic molecule properties and the corrosion hindrance on mild steel surface [30]. In this paper, DFT was operated utilizing B3LYP with a basic 6–31 G/(d,p) process with Gaussian 09 programming. The quantum descriptors, for example, the fraction of electrons transferred from the inhibitor compound to the metal surface ( $\Delta N$ ), softness ( $\sigma$ ), LUMO and HOMO energy, total energy ( $E_{\text{total}}$ ), dipole moment ( $\mu$ ), electronegativity ( $\chi$ ), global electrophilicity index ( $\omega$ ), and global hardness ( $\eta$ ), which may be obtained through the following equations, where  $\eta_{\text{Fe}} = 0$  and  $\chi = 7$  eV [35]:

$$\Delta E = E_{\text{LUMO}} - E_{\text{HOMO}} \quad (15)$$

$$\chi = -\frac{1}{2}(E_{\text{HOMO}} + E_{\text{LUMO}}) \quad (16)$$

$$\eta = -\frac{1}{2}(E_{\text{HOMO}} - E_{\text{LUMO}}) \quad (17)$$

$$\sigma = \frac{1}{\eta} \quad (18)$$

$$\Delta N = \frac{\chi(\text{Fe}) - \chi(\text{inh})}{2(\eta(\text{Fe}) + \eta(\text{inh}))} \quad (19)$$

$$\omega = \frac{\chi^2}{2\eta} \quad (20)$$

### 3.6. Global Molecular Reactivity of Urea Molecule

The quantum descriptors of urea inhibitors in the non-aqueous and aqueous phases are grouped in Table 5. The urea inhibitor has the lowest  $E_{\text{LUMO}}$  value, which demonstrates

the ability of this inhibitor to acquire electrons in the aqueous phase [36]. In the aqueous phase, its energy gap ( $\Delta E$ ) is low, 5.0241 eV; hence, the reactivity of the urea in the aqueous environment is higher [37]. The fraction electrons transferred ( $\Delta N$ ) value is under 3.6, which demonstrates that the inhibitor molecule has a tendency to give electrons to the metal surface [34]. This outcome shows that an increase in the electron-donating potential to the mild steel can prompt an increment in the inhibitory impact on the mild steel by the urea inhibitor. However, the dipole moment value (5.3282 D) shows that the inhibitor progressively became polar, so it effectively donates electrons and creates a thin protective organic layer on the mild steel surface when in contact with the aqueous medium [38]. The outcomes show similar progress in the two stages (aqueous and nonaqueous phases).

**Table 5.** Quantum descriptors of urea inhibitor studied.

Descriptors	$E_{\text{HOMO}}$ (eV)	$E_{\text{LUMO}}$ (eV)	$\Delta E$ (eV)	$\eta$	$\sigma$ (eV <sup>-1</sup> )	$\Delta N$	$\chi$	$\omega$	$\mu$ (D)	Total Energy (u.a)
Urea (Gas phase)	-6.7187	-1.5885	5.1302	5.9244	0.1688	0.2364	4.1536	1.4561	4.2487	-225.2716
Urea (Aqueous phase)	-7.0176	-1.9935	5.0241	6.0208	0.1661	0.2071	4.5055	1.6858	5.3282	-225.2845

### 3.6.1. HOMO and LUMO

The HOMO and LUMO electron density distribution of urea, as shown in Figure 6, illustrates the orbitals occupied by the electrons. The red shows higher electron concentration in that place and green indicates electron deficiency in that region [39]. The HOMO and LUMO orbitals electron density indicate that the urea inhibitor can send electrons to the vacant d orbital of the Fe [40]. On the other hand, the geometry plane of this inhibitor shows its ability to adsorb on the surface of the mild steel by the formation of chemical or electrostatic bonds [41].

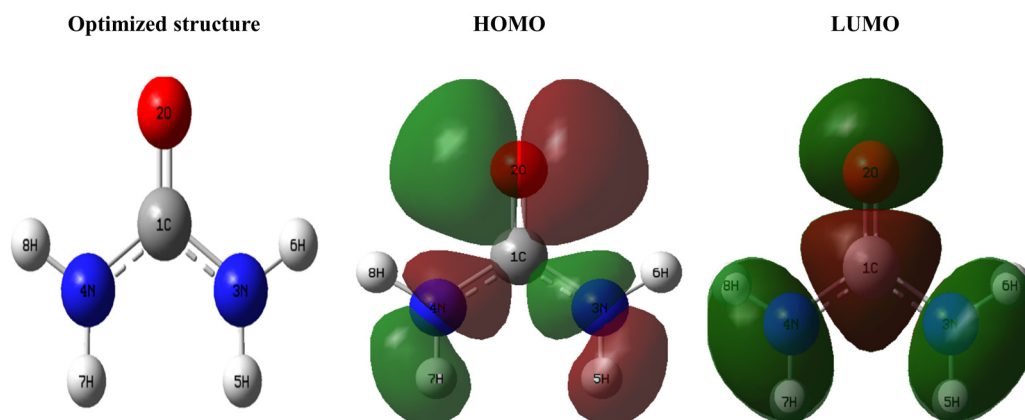


**Figure 6.** Optimized molecular structure and electron density distributions of urea inhibitor.

### 3.6.2. Fukui Function of Urea Inhibitor in Aqueous Phase

The Fukui values are determined in view of the number of inhabitants in every molecule in various species, cationic, anionic, and neutral species, using the following equations [42]:

$$F_k^+ = P_k(N+1) - P_k(N) \quad (21)$$

$$F_k^- = P_k - P_k(N-1) \quad (22)$$

$$F_k^0 = P_k(N+1) - P_k(N-1) \quad (23)$$

With  $P_k(N+1)$ ,  $P_k(N)$ , and  $P_k(N-1)$  as the natural populations for the atom  $k$  in the anionic, neutral, and cationic species, respectively.

From the calculated Fukui indices, as shown in Table 6, the majority of the sites of the studied reagents were nucleophiles shown in O2, N3, and N4 heteroatoms. These results indicate the inhibitory capability of urea when studied in an aqueous solution.

**Table 6.** Fukui values of urea inhibitor examined by B3LYP/6–31G in the aqueous phase.

Atoms	P(N)	P(N + 1)	P(N – 1)	$F_k^+$	$F_k^-$	$F_k^0$
C1	5.1960	5.2084	5.2655	0.0124	−0.0695	−0.0571
O2	8.7322	8.7640	8.6104	0.0318	0.1218	0.1536
N3	7.8990	7.9370	7.5106	0.038	0.3884	0.4264
N4	7.8990	7.9370	7.5106	0.038	0.3884	0.4264

### 3.6.3. Monte Carlo Simulation

The aim of this study was to examine the conceivable adsorption of urea within the sight of water on the mild steel corrosion utilizing Monte Carlo calculations [42]. Figure 7 shows the most stable configuration associated with the low adsorption energy of examined inhibitor molecules on Fe(110). As a rule, adsorption is the process of corrosion inhibition [43]. This outcome depends on the higher negative value of adsorption energy attributed to good adsorption behavior with the most stable configuration (Table 7). The inhibitory value is expanded by the presence of water, demonstrating the steric impact and the extent of the electronic density of donor atoms engaged in the inhibitor molecule concerning their key function in the adsorption process. Subsequently, the adsorption energy of inhibitory molecules is higher than that acquired with water molecules. This clarifies the chance of trading water molecules on mild steel, as the steady interaction is intended to shield mild steel from corrosion in the corrosive media [44].

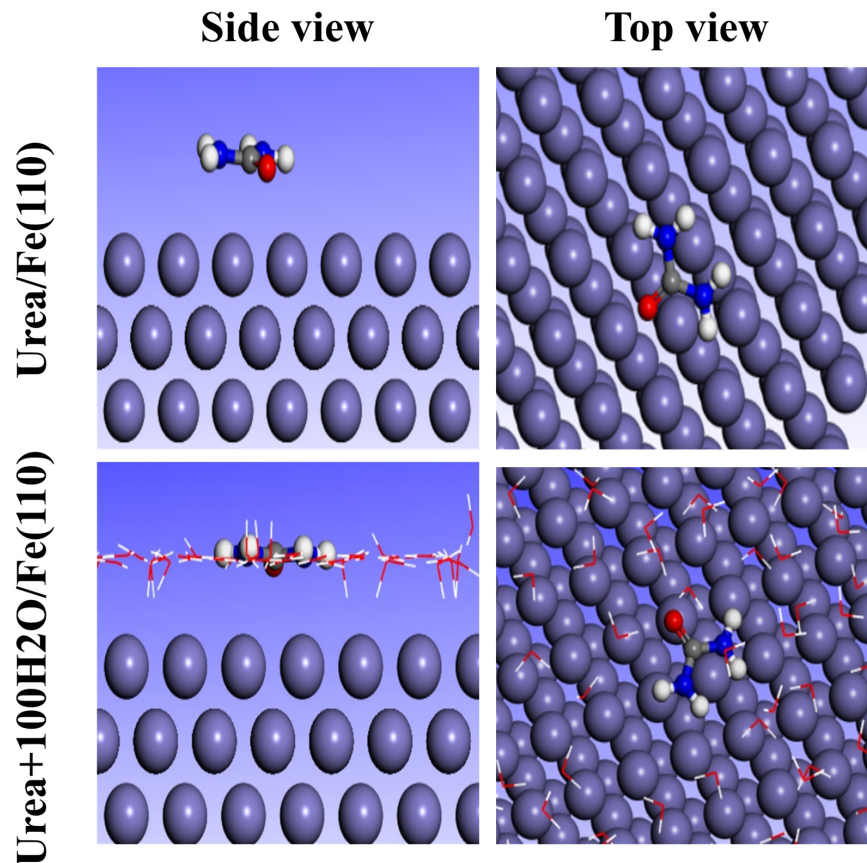


**Figure 7.** The highest stable configuration for the adsorption of urea molecule on the Fe(110) surface was achieved utilizing the Monte Carlo simulation.

**Table 7.** The adsorption energy of the examined inhibitor molecules on the Fe(110) surface utilizing the Monte Carlo simulation (kcal/mol).

Systems	Adsorption Energy Inhibitor	Adsorption Energy Water
Fe(110)/urea	−24.78	-
Fe(110)/urea/100H <sub>2</sub> O	−1567.98	−15.63

#### 4. Conclusions

Significant results were found in the experimental results. Urea acts as a disinfectant on mild steel when immersed in AGO media. The inhibition efficiency ranges from 69.30 to 10.395 with a rise in immersion time. The longer the immersion time, the lower the inhibition efficiency. The inhibitor exhibited poor protection against corrosion in AGO media, in which the major setback was the time dependence of percentage inhibition efficiency of the tested inhibitor. The adsorption of urea on mild steel follows Frumkin's adsorption isotherm. Free adsorption energy reflects the physical and electrostatic interactions between the urea inhibitor and the surface of the mild steel. The poor inhibitory effect of the inhibitor suggests dissolution of the adsorbed inhibitor molecule on the surface of the mild steel as immersion time progresses. SEM and EDX confirmed the poor surface protection performance by the urea on the mild steel surface in the AGO environment. The theoretical outcomes showed the inhibition performance of urea on the mild steel surface but the results obtained in these study indicate that oxygen and nitrogen atoms did not positively influence its efficiency over inhibition of mild steel in AGO media. The theoretical findings in the current investigation were not in agreement with the experimental result. Based on these findings from the gasometric results, a clearer adsorption and inhibition performance of urea on the mild steel in AGO media needs to be studied further using an electrochemical method.

**Author Contributions:** N.E.C.: writing—original draft, conceptualization, investigation, visualization. R.H.; writing—original draft, conceptualization, investigation visualization (equal contribution). U.K.G. and O.C.C.: reviewing and editing paper. E.A.U. and O.P.I.: methodology, software, validation. M.O.O., H.I. and M.T.; methodology, validation. O.D. and E.E.E.; computational. N.A. and S.-C.K.: conceptualization, visualization. All authors have read and agreed to the published version of the manuscript.

**Funding:** This research was funded by the Nigerian Tertiary Education Trust Fund (TETFund) through Institution Based Research (IBR) Project Grant 2019, grant number TETFUND/DRSS/PoLY/NEKEDE/2014/RP/Vol.1.

**Data Availability Statement:** Not applicable.

**Acknowledgments:** The authors acknowledge the TETFund for its financial support. The authors are also grateful to the Department of Chemistry and Management of Federal Polytechnic Nekede, Owerri-Imo State for providing research facilities for the research work.

**Conflicts of Interest:** The authors declare no conflict of interest.

#### References

- Kolawale, F.O.; Kolawale, S.K.; Agunsonye, J.O.; Adebisi, J.A.; Bello, S.A.; Hassan, S.B. Mitigation of corrosion problems I API5L steel pipeline: A review. *J. Mater. Environ. Sci.* **2018**, *9*, 2397–2410.
- Fajobi, M.A.; Loto, T.R.; Oluwole, O.O. Corrosion in crude distillation overhead system: A review. *J. Bio-Tribo-Corros.* **2019**, *5*, 67. [[CrossRef](#)]
- Fajobi, M.A.; Loto, T.R.; Oluwole, O.O. Austentic 316L stainless steel; corrosion and organic inhibitor: A review. *Key Eng. Mater.* **2021**, *886*, 126–132. [[CrossRef](#)]
- Tamalmani, K.; Husin, H. Review on corrosion inhibitors for oil and gas corrosion issues. *Appl. Sci.* **2020**, *10*, 3389.
- Obanijesu, E.O.; Pareek, V.; Gubner, R.; Tade, M.O. Corrosion education as a tool for the survival of natural gas industry. *NAFTA* **2010**, *61*, 541–554.
- Rajeev, P.; Surendranathan, A.O.; Murthy, C.S.N. Corrosion mitigation of the oil well steels using organic inhibitors—A Review. *J. Mater. Environ. Sci.* **2012**, *3*, 856–869.

7. Al Sultani, K.F.; Al Roubaiby, A.O.; Duaa, A.A. Characterization of corrosion behavior of low carbon steel oil pipelines by crude oil. *Res. J. Recent Sci.* **2016**, *5*, 7–13.
8. Papoola, L.T.; Grema, A.S.; Latinwo, G.K.; Gutti, B.; Balogun, A.S. Corrosion problems during oil and gas production and its mitigation. *Int. J. Ind. Chem.* **2013**, *4*, 1–15.
9. Perez, T.E. Corrosion in the oil and gas industry: An increasing challenge for materials. *JOM* **2013**, *65*, 1033–1042. [[CrossRef](#)]
10. Olvera-Martinez, M.E.; Mendoza-Flores, J.; Genesca, J. CO<sub>2</sub> corrosion control in steel pipelines: Influence of turbulent flow on the performance of corrosion inhibitors. *J. Loss Prev. Process Ind.* **2015**, *35*, 19–28.
11. Asmara, Y.P. The roles of H<sub>2</sub>S gas in behaviour of carbon steel corrosion in oil and gas environment: A review. *J. Tek. Mesin.* **2018**, *7*, 37–43.
12. Kahyarian, A.; Achour, M.; Nesic, S. CO<sub>2</sub> corrosion of mild steel. In *Trends in Oil and Gas Corrosion Research and Technologies*; Elsevier: Amsterdam, The Netherlands, 2015; pp. 149–190.
13. Ezeibe, A.U.; Nleonu, E.C.; Ahumonye, A.M. Thermodynamics study of inhibitory action of lignin extract from *Gmelina arborea* on the corrosion of mild steel in dilute hydrochloric acid. *Int. J. Sci. Eng. Res.* **2019**, *7*, 133–136.
14. Ezeibe, A.U.; Onyemenonu, C.C.; Nleonu, E.C.; Onyema, A.V. Corrosion inhibition performance of safranin towards mild steel in acidic corrosion. *Int. J. Sci. Eng. Res.* **2019**, *10*, 1539–1544.
15. Verma, D.K.; Aslam, R.; Aslam, J.; Quraishi, M.A.; Ebenso, E.E.; Verma, C. Computational modeling: Theoretical predictive tools for designing of potential organic corrosion inhibitors. *J. Mol. Struct.* **2021**, *1236*, 1–22.
16. Rosli, N.R.; Yusuf, S.M.; Sauki, A.; Razali, W.M.R.W. *Musa sapientum* (Banana) peels as green corrosion inhibitor for mild steel. *Key Eng. Mater.* **2019**, *797*, 230–239. [[CrossRef](#)]
17. Verma, C.; Olasunkanmi, L.O.; Ebenso, E.E.; Quraishi, M.A.; Obot, I.B. Adsorption behavior of glucosamine—Based, pyrimidine fused heterocycles as green corrosion inhibitors for mild steel: Experimental and theoretical studies. *J. Phys. Chem. C* **2016**, *120*, 11598–11611.
18. Charitha, B.P.; Rao, P. An ecofriendly approach for corrosion control of 6061 Al-15%(v) SiC(P) composite and its base alloy. *Chin. J. Chem. Eng.* **2017**, *25*, 363–372.
19. Finšgar, M.; Jackson, J. Application of corrosion inhibitors for steels in acidic media for the oil and gas industry: A review. *Corros. Sci.* **2014**, *86*, 17–41.
20. Ubaka, K.G.; Mong, o.o.; Nleonu, E.C. Investigation of inhibitory effect of thiourea on corrosion of mild steel in dual purpose kerosene (DPK) and premium motor spirit (PMS). *Int. J. Adv. Eng. Manag.* **2020**, *2*, 162–168.
21. Goyal, M.; Kumar, S.; Bahadur, I.; Verma, C.; Ebenso, E. organic corrosion inhibitors for industrial cleaning of ferrous and non-ferrous metals in acidic solutions: A review. *J. Mol. Liq.* **2018**, *256*, 563–573.
22. Ayuba, A.M.; Abubakar, M. Computational study for molecular properties of some of the isolated chemicals from leaves extract of *Guiera senegalensis* as aluminium corrosion inhibitor. *J. Sci. Technol.* **2021**, *13*, 47–56. [[CrossRef](#)]
23. Arrousse, N.; Mabrouk, E.; Ismaily Alaoui, K.; El hajjaji, F.; Rais, Z.; Taleb, M. Economical and new synthesis strategy, characterization and theoretical study of 3-oxo-3H-spiro [isobenzofuran-1,9'-xanthene]-3',6'-diyl dibenzoate. *SN Appl. Sci.* **2020**, *2*, 1–12. [[CrossRef](#)]
24. Verma, C.; Saji, V.S.; Quraishi, M.A.; Ebenso, E.E. Pyrazole derivatives as environmental benign acid corrosion inhibitors for mild steel: Experimental and computational studies. *J. Mol. Liq.* **2020**, *298*, 111943. [[CrossRef](#)]
25. Shehu, N.U.; Gaya, U.I.; Muhammad, A.A. Influence of side chain on the inhibition of aluminium corrosion in HCl by  $\alpha$ -amino acids. *Appl. Sci. Eng. Progr.* **2019**, *12*, 186–197. [[CrossRef](#)]
26. Abdellaoui, O.; Skalli, M.K.; Haoudi, A.; Kandri Rodi, Y.; Arrousse, N.; Taleb, M.; Ghibate, R.; Senhaji, O. Study of the inhibition of corrosion of mild steel in a 1M HCl solution by a new quaternary ammonium surfactant. *Mor. J. Chem.* **2021**, *9*, 44–56. [[CrossRef](#)]
27. Alaoui Mrani, S.; Ech-chihbi, E.; Arrousse, N.; Rais, Z.; El Hajjaji, F.; El Abiad, C.; Radi, S.; Mabrouki, J.; Taleb, M.; Jodeh, S. DFT and Electrochemical Investigations on the Corrosion Inhibition of Mild Steel by Novel Schiff's Base Derivatives in 1M HCl Solution. *Arab. J. Sci. Eng.* **2021**, *46*, 5691–5707. [[CrossRef](#)]
28. Ayuba, A.M.; Uzairu, A.; Abba, H.; Shallangwa, G.A. Hydroxycarboxylic acids as corrosion inhibitors on aluminium metal: A computational study. *J. Mater. Environ. Sci.* **2018**, *9*, 3026–3034.
29. Aluvihara, S.; Premachandra, J.K. Fundamental corrosive properties of crude oils and their effects on the ferrous metals. *J. Chem. Eng. Process Technol.* **2018**, *9*, 1–7.
30. Undiandeye J, A.; Choir, T.J.; Mohammed, A.; Offurum, J.C. Kinetics of the corrosion of mild steel in petroleum-water mixtures using ethyl ester of lard as inhibitor. *AU J. Technol.* **2014**, *17*, 129–136.
31. Arrousse, N.; Nahlé, A.; Mabrouk, E.; Salim, R.; El hajjaji, F.; Rais, Z.; Taleb, M. An Intelligent and Efficient Synthesis of New Inhibitors against Corrosion of Mild Steel in Acidic Media. *Surf. Eng. Appl. Electrochem.* **2021**, *57*, 136–147. [[CrossRef](#)]
32. Chafiq, M.; Chaoui, A.; Al-Hadeethi, M.R.; Ali, I.H.; Mohamed SKToumiat, K.; Salghi, R. Naproxen-based hydrazones as effective corrosion inhibitors for mild steel in 1.0 M HCl. *Coatings* **2020**, *10*, 700. [[CrossRef](#)]
33. Al-Amiery, A.A.; Isahak, W.N.R.W.; Takriff, M.S. Inhibition of mild steel corrosion by 4-benzyl-1-94-oxo-4-phenylbutanoyl)thiosemicarbazide. Gravimetric, adsorption and theoretical studies. *Lubricants* **2021**, *9*, 93. [[CrossRef](#)]
34. Arrousse, N.; Mabrouk, E.; Hammouti, B.; El hajjaji, F.; Rais, Z.; Taleb, M. Synthesis, Characterization, anti corrosion behaviour and theoretical study of the new organic dye: 3-oxo-3H-spiro[isobenzofuran-1,9'-xanthene]-3',6'-diyl bis(3-methylbenzenesulfonate). *Int. J. Corros. Scale Inhib.* **2020**, *9*, 661–687.

35. Fernine, Y.; Ech-chihbi, E.; Arrousse, N.; El Hajjaji, F.; Bousraf, F.; EbnTouhami, M.; Rais, Z.; Taleb, M. Ocimum basilicum seeds extract as an environmentally friendly antioxidant and corrosion inhibitor for aluminium alloy 2024 -T3 corrosion in 3 wt % NaCl medium. *Colloids Surf. A Physicochem. Eng. Asp.* **2021**, *627*, 127232. [[CrossRef](#)]
36. Saady, A.; El-Hajjaji, F.; Taleb, M.; Ismaily Alaoui, K.; El Biache, A.; Mahfoud, A.; Alhouari, G.; Hammouti, B.; Chauhan, D.S.; Quraishi, M.A. Experimental and theoretical tools for corrosion inhibition study of mild steel in aqueous hydrochloric acid solution by new Indanones derivatives. *Mater. Discov.* **2019**, *217*, 1230–1242.
37. Lazrak, J.; Salim, R.; Arrousse, N.; Ech-chihbi, E.; El-Hajjaji, F.; Taleb, M.; Farah, A.; Ramzi, A. Mentha viridis oil as a green effective corrosion inhibitor for mild steel in 1 M HCl medium. *Int. J. Corros. Scale Inhib.* **2020**, *9*, 1580–1606. [[CrossRef](#)]
38. Mohamed, A.M.M.; Elmsellem, H.; Benchidmi, M.; Sebbar, N.K.; Belghiti, M.A.; El ouasif, L.; Jilalat, A.E.; Kadmi, Y.; Essassi, E.M. A DFT and Molecular Dynamics Study on Inhibitory Action of indazole Derivative on Corrosion of Mild Steel. *JMES* **2017**, *8*, 1860–1876.
39. Zaidi, S.Z.; Hassan, S.; Raza, M.; Walsh, F.C. Transition metal oxide as possible electrode materials for Li-ion batteries: A DFT Analysis. *Int. J. Electrochem. Sci.* **2021**, *16*, 1–10.
40. Arrousse, N.; Mabrouk, E.; Salim, R.; Ismaily alaoui, K.; El Hajjaji, F.; Rais, Z.; Taleb, M.; Hammouti, B. Fluorescein as commercial and environmentally friendly inhibitor against corrosion of mild steel in molar hydrochloric acid medium. *Mater. Today Proc.* **2020**, *27*, 3184–3292.
41. Obot, I.B.; Haruna, K.; Saleh, T.A. Atomistic Simulation: A Unique and Powerful Computational Tool for Corrosion Inhibition Research. *Arab. J. Sci. Eng.* **2019**, *44*, 1–32.
42. Arrousse, N.; Salim, R.; Kaddouri, Y.; Abdelkader, Z.D.Z.; El Hajjaji, F.; Touzani, R.; Taleb, M.; Jodeh, S. The inhibition behavior of Two pyrimidine-pyrazole derivatives against corrosion in hydrochloric solution: Experimental, surface analysis and in silico approach studies. *Arab. J. Chem.* **2020**, *12*, 5949–5965.
43. Arrousse, N.; Salim, R.; Benhiba, F.; Mabrouk, E.H.; Abdelaoui, A.; El-Hajjaji, F.; Warad, I.; Zarrouk, A.; Taleb, M. Insight into the corrosion inhibition property of two new soluble and non-toxic xanthenbenzoate derivatives. *J. Mol. Liq.* **2021**, *338*, 116610.
44. Arrousse, N.; Salim, R.; Abdellaoui, A.; El hajjaji, F.; Hammouti, B.; Wilson, A.D.; Mabrouk El Taleb, M. Synthesis, characterization, and evaluation of xanthene derivative as highly effective. nontoxic corrosion inhibitor for mild steel immersed in 1 M HCl solution. *J. Taiwan Inst. Chem. Eng.* **2021**, *120*, 344–359. [[CrossRef](#)]